Model Predictive Control-based Power take-off Control of an Oscillating Water Column Wave Energy Conversion System

2017 IOP Conf. Ser.: Earth Environ. Sci. 73 012010

(http://iopscience.iop.org/1755-1315/73/1/012010)

IOP Conf. Series: Earth and Environmental Science **73** (2017) 012010 doi:10.1088/1755-1315/73/1/012010

Model Predictive Control-based Power take-off Control of an Oscillating Water Column Wave Energy Conversion System

G Rajapakse[1], S G Jayasinghe[1], A Fleming[1] and F Shahnia[2]
[1] Australian Maritime College, University of Tasmania, Australia
[2] School of Engineering and Information Technology, Murdoch University, Australia

Email: Gimara.rajapakse@utas.edu.au

Abstract: Australia's extended coastline asserts abundance of wave and tidal power. The predictability of these energy sources and their proximity to cities and towns make them more desirable. Several tidal current turbine and ocean wave energy conversion projects have already been planned in the coastline of southern Australia. Some of these projects use air turbine technology with air driven turbines to harvest the energy from an oscillating water column. This study focuses on the power take-off control of a single stage unidirectional oscillating water column air turbine generator system, and proposes a model predictive control-based speed controller for the generator-turbine assembly. The proposed method is verified with simulation results that show the efficacy of the controller in extracting power from the turbine while maintaining the speed at the desired level.

1. Introduction

The climate change, pollution, scarcity and various other negative aspects of conventional fossil fuels advocate the growth of clean energy technologies such as solar, wind, ocean, bio-fuel, etc. Out of these, ocean energy has drawn much attention in recent years as one of the most promising renewable energy resources with high energy density and low cost [1]-[2]. More than 70% of the earth is covered by oceans that have a vast amount of renewable energy, stored as thermal, potential and kinetic energies. These ocean energies also consist of unique characteristics; vast, sustainable and almost zero environmental impact [1],[3]. It has been proven that tidal current is very predictable and the tidal charts are accurate for years to come and the wave energy can be predicted several days in advance [4]. These characteristics permit both of these energies to be used for supplying the base power demand mixed with other appropriate generation and/or storage systems [1]. According to [4], the ocean energy available in less than 80m depth from ocean connected coastlines is almost 5 times the world consumption which is approximately 15PWh per annum. However, at present, ocean energy supplies only 0.02% of the world energy consumption.

One challenge for wave and tidal energy is to generate electricity at a constant level. On average, tidal current speed drops to zero twice in every 12.4 hours (time varies according to the location) and the speed varies depending on the proximity of the moon and sun relative to earth, despite its independency from prevailing weather conditions [1],[5]. In contrast, wave swell depends on the wind speed, duration of wind, as well as the depth and topography of the sea floor [1]. The length and strength of waves vary from one to the next, leading to time varying generation of power from the

waves. Therefore, the inherent variability of marine kinetic energy requires some form of energy storage for smooth generation of electrical power.

Another main challenge is economic feasibility as the high production cost at present challenges the large-scale commercial applications. At this stage, in Australia, wave and tidal energies are at the pre-commercial state and their outlook depends on research, development, and demonstration [1],[2],[3]. According to [3], there are several ocean energy demonstration plants operating or under construction in the coastline of Southern Australia. Most of these projects are based on wave energy conversion systems (WECs). The companies involved in these projects believe their nearshore shallow water ocean renewable energy projects could be cost competitive with other onshore renewables and fossil fuels in coming years [4],[6],[7].

The WECs engaged in different projects employ different conversion principles. These systems could be categorized into three main groups; oscillating bodies (Attenuator), oscillating water column (OWC) and overtopping device [3], [8]. The principle of oscillating bodies converts the kinetic energy of the wave into mechanical energy by absorbing the wave energy to induce an alternating motion on a structure immersed in the ocean. This motion operates the hydraulic cylinder to extend and retract. The high-pressure oil produced as a result of this motion drives a generator [9], [10]. The project in Garden Island by Carnegie Wave Energy employs CETO wave converter; fully submerged buoy with CETO pod, comes under Oscillating bodies. The project by BioPower Systems in Port Fairy uses similar principle with BioWAVE concept and O-Drive module [3]. The OWC principle is based on the oscillating motion of the water that is used to compress air inside a chamber and direct the air into an air turbine. The turbine is then coupled with a generator [4], [6]-[8]. The King Island project by Wave Swell energy uses the OWC principle. The overtopping principle is based on the use of a hydraulic head between a reservoir and the mean water level to drive turbines. This technology is not yet used in any project in Australia.

Irregular natural behavior of ocean waves creates irregular air flow inside the OWC chamber which is then passed onto the turbine. Consequently, the speed of the generator coupled to the turbine also varies, resulting in variable voltage and/or frequency at the output. Therefore, to interface this variable output of the generator into the ac grid, a rectifier-inverter combination is required. If the grid is dc only, a rectifier is required to extracts power from the turbine-generator assembly and feed into the grid. Therefore, irrespective of the grid type, speed control of the turbine is carried out by a rectifier, either to one or different speed levels to maintain the turbine speed at an optimum level to uphold maximum efficiency of the turbine.

This paper focuses on the speed control of the turbine through the control of the rectifier while feeding power to a dc grid. The traditional approach in generator speed control is to employ proportional-integral (PI) controllers which require careful tuning to achieve desired performance. This paper takes a novel approach to use the model predictive control (MPC). The particular turbine considered in this study has a unidirectional airflow through it and produces power only during the air intake. Moreover, it does not essentially require variable speed operation and thus, a constant speed of 650rpm is set as the control objective while extracting power from the waves.

As the focus of this paper is on the electrical power take off from the turbine, modeling and analysis of airflow inside the OWC and torque generation of the turbine are not discussed. Instead, a typical torque profile produced by the turbine at 650rpm is considered as the mechanical input to the generator. As the torque varies, the input power to the generator varies and thus, the rectifier has to change its power extraction while maintaining the speed. This control objective is applied to the

proposed controller which predicts the speed in the next sampling interval for all the switching combinations of the rectifier and selects the combination with the lowest speed error. As this particular controller is based on the system model and does not require tuning, it is fast and simple to use.
The rest of the paper is organized as follows. Section 2 explains the operation of the OWC air turbine. Section 3 presents the mathematical model of the generator assembly followed by the MPC of the rectifier in Section 4. Section 5 presents the simulations results to verify the operation of the proposed MPC strategy. Conclusions drawn from this study are presented in the Section 6.

2. OWC air turbine system

The majority of the WECs, which are based on offshore underwater locations, require the entire system to be lifted above the sea level or use divers to carry out maintenance and repairs which is very costly. Therefore, at present, much research is in progress to develop topologies to find the best solutions to maximize efficiency and robustness while minimizing the overall size of the turbine, generator, converters, repair and maintenance cost, etc. [6],[7] [8]. The OWC air turbine system has relatively easy access particular to the energy conversion system since the turbine, generator and associated parts are well above the water line. This design not only allows regular maintenance but is also a cost-effective power generation option.

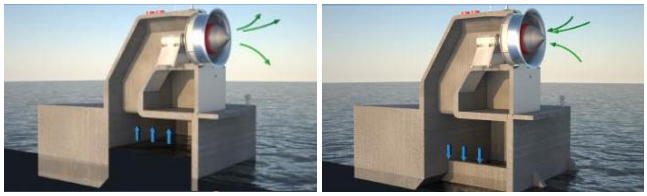

Figure 1. OWC bidirectional air turbine [6].

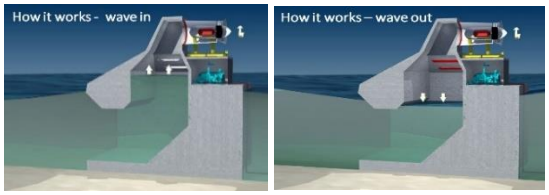

Figure 2. OWC Unidirectional air turbine [7].

The air turbine technologies such as Impulse, Radial, etc. are currently being researched to gain better overall performance at irregular flow conditions and avoid stall which is a drawback of the Wells turbine technology [11]. Regardless of the type of air turbine deployed, the overall design of OWC-based WECs are based on the rise and fall of the ocean wave in a partially submerged chamber. The arrangement is in a way that when the passing wave oscillates inside the WEC chamber oscillates the trapped air inside the chamber. The air pressure fluctuation inside the chamber forces the air to pass in/out through an air turbine at the top of the chamber. The turbine is coupled to a generator. The rotational speed of the turbine depends on the air pressure and the control system of the generator.
As shown in Figure 1, the Oceanlinx's OWC turbine has employed the bidirectional reaction turbine for continuous electricity generation in varying flow conditions and flow directions of the waves [6]. As shown in Figure 2, the Wave Swell Energy uses unidirectional air turbine with ingenious concept and allows to use simpler, robust and more reliable design targeting to achieve higher energy conversion efficiency [7]. This study considers only the single stage unidirectional air turbine to model the drive system of the generator. The single stage unidirectional air turbines are designed to harness only omnidirectional airflow. These types of turbines are free from limitations due to stalling compared to bidirectional turbines. Moreover, they provide useful efficiencies over wide range of flow rates; thus, they are capable of operating over wide range of pressure drop conditions; increase the pressure drop with increasing flow rate till they become choked preventing further increase with increasing flow rate at much higher pressure drop away from range of interest [12]. In this study, a

typical torque profile of the abovementioned turbine is used as the mechanical input to the generator [7].

3. Mathematical model of the generator

The proposed electrical power conversion system is designed to extract power from the turbine, exploiting the simple and most appropriate subsystems that suits to the OWC air turbine system. The system utilizes a three-phase permanent magnet synchronous generator (PMSG) and a two-level active front-end (AFE) rectifier built with insulated gate bipolar transistors (IGBTs). An MPC technique controls the rectifier. Figure 3 illustrates the considered PMSG connected to the dc interface system.

Even though a multi-pole PMSG is a comparatively large and heavy machine, it has the advantage of using direct drive system avoiding gears. Moreover, it has the ability to use full speed range and requires no power converter or brushes to supply and control the field winding. Therefore, PMSGs are robust and require low maintenance. [13],[14],[15],[16]. Many researchers also believe that, this improved reliability of the system due to reduced mechanical stresses and low maintenance cost would compensate the initial cost [13],[14],[17]. Therefore, a PMSG is chosen as the generator in this study. The active and reactive power of the generator output in the $\alpha\beta$ reference frame, assuming a balanced three-phase system, are given as [18];

$$P = v_{s\alpha} i_{s\alpha} + v_{s\beta} i_{s\beta} \quad (1)$$

$$Q = v_{s\beta} i_{s\alpha} - v_{s\alpha} i_{s\beta} \quad (2)$$

where P and Q are the active and reactive power respectively, v_s and i_s are the source voltage and current respectively while subscripts $_\alpha$ and $_\beta$ represent the real and imaginary axes. The space vector models of

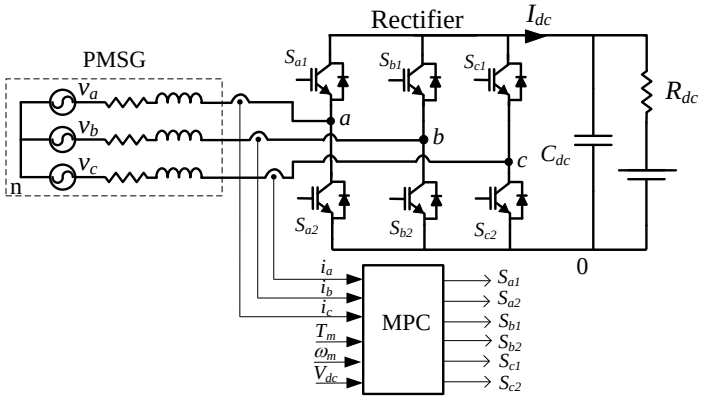

Figure 3. OWC Air turbine generator – dc grid interface system.

the three-phase source voltage ($\vec{v_s}$) and source current ($\vec{i_s}$) derived from the phase voltages (v_{sa}, v_{sb}, v_{sc}), and currents (i_{sa}, i_{sb}, i_{sc}) can be represented as in (3) and (4) where $\vec{\omega} = e^{\frac{j2\pi}{3}}$ [19].

$$\vec{v}_s = \frac{2}{3}\left(v_{sa} + \vec{\omega} v_{sb} + \overrightarrow{\omega^2} v_{sc}\right) \quad (3)$$

$$\vec{i}_s = \frac{2}{3}\left(i_{sa} + \vec{\omega} i_{sb} + \overrightarrow{\omega^2} i_{sc}\right) \quad (4)$$

The mathematical model of the variable speed multi-pole PMSG in the dq synchronous rotating reference frame, assuming symmetrical stator windings, negligible stator slots' effect on the rotor

inductances with rotor position, negligible magnetic hysteresis and saturation effects, and constant power losses in windings can be given by [2], [20].

$$v_{sd} = R_s i_{sd} + L_d \frac{di_{sd}}{dt} - \omega_e L_q i_{sq} \quad (5)$$

$$v_{sq} = R_s i_{sq} + L_q \frac{di_{sq}}{dt} + \omega_e L_d i_{sd} + \omega_e \Psi_{pm} \quad (6)$$

while the PMSG's flux and electromagnetic torque are

$$\Psi_{sd} = L_d i_{sd} + \Psi_{pm}; \quad \Psi_{sq} = L_q i_{sq} + 0 \quad (7)$$

$$T_e = 1.5 n_p \left[\left(L_d - L_q \right) i_{sd} i_{sq} + \Psi_{pm} i_{sq} \right] = 1.5 n_p \Psi_{pm} i_q \quad (8)$$

Rewriting (1) and (2) in the *dq* synchronous rotating reference frame, one gets

$$P = T_e \omega_m = 1.5 \left(v_{sd} i_{sd} + v_{sq} i_{sq} \right) \quad (9)$$

$$Q = 1.5 \left(v_{sq} i_{sd} - v_{sd} i_{sq} \right) \quad (10)$$

where i_{sd} and i_{sq} are the physical current quantities transformed into the dq frame, v_{sd} and v_{sq} are the physical voltage quantities transformed into the dq frame, R_s is the stator's resistance, $L_d = L_q$ are the inductances of the PMSG on the dq axis, Ψ_{pm} is the permanent magnet flux, Ψ_{sd} and Ψ_{sq} are the flux components respectively in the *d* and *q* axes, T_e is the generator's electromagnetic torque, and ω_m is the mechanical angular speed of the generator.

The formulas associated with the turbine and generator rotor, considering the direct drive system of the turbine generator and zero rotational damping coefficient can be written as;

$$J \frac{d\omega_m}{dt} = T_m - T_e \quad (11)$$

Where $J = J_e + \frac{J_t}{n_g}$

The generator rotor electrical angular speed (ω_e) can be written as

$$\omega_e = n_p \omega_m = 2\pi f_e \quad (12)$$

where J_e , J_t and J are the inertia of the generator, turbine and the air turbine system respectively, T_m is the mechanical torque of the turbine, n_g is the gear ratio, n_p is the number of pole pairs, and f_e is the electric frequency.

4. AFE rectifier and MPC of the converter

4.1. AFE Converter Model

The rectifier consists of 6 IGBT-diode switches. The circuit is fed by the ac voltage (v_s), generated by the PMSG, through combination of source and line filter inductances L_s = [(L_{sa} +L_{fa}), (L_{sb} +L_{fb}), (L_{sc} +L_{fc})]^T and resistances R_s = [(R_{sa} +R_{fa}), (R_{sb} +R_{fb}), (R_{sc} +R_{fc})]^T. A dc-link capacitor (C_{dc}) reduces the voltage ripples. The IGBT switches operate in such a manner that two IGBTs connected to the same phase are operated in contrary mode to avoid short circuits (e.g., when S_{a1} is ON, S_{a2} is OFF, and vice versa). The rectifier's switching state is determined by the gating signals S_a, S_b and S_c. These three switching signals can produce eight consequent switching states resulting in eight possible voltage vectors as presented in Table 1 and Figure 4.

Table 1. Switching states and voltage space vectors [15],[19]

Switching states			Voltage space vector
S_a	S_b	S_c	$\overrightarrow{V_{AFE}}$
0	0	0	$\overrightarrow{V_0} = 0$
1	0	0	$\overrightarrow{V_1} = 2V_{dc}/3$
1	1	0	$\overrightarrow{V_2} = V_{dc}/3 + \mathrm{j}\, V_{dc}/\sqrt{3}$
0	1	0	$\overrightarrow{V_3} = -V_{dc}/3 + \mathrm{j}\, V_{dc}/\sqrt{3}$
0	1	1	$\overrightarrow{V_4} = -2V_{dc}/3$
0	0	1	$\overrightarrow{V_5} = -V_{dc}/3 - \mathrm{j}\, V_{dc}/\sqrt{3}$
1	0	1	$\overrightarrow{V_6} = V_{dc}/3 - \mathrm{j}\, V_{dc}/\sqrt{3}$
1	1	1	$\overrightarrow{V_7} = 0$

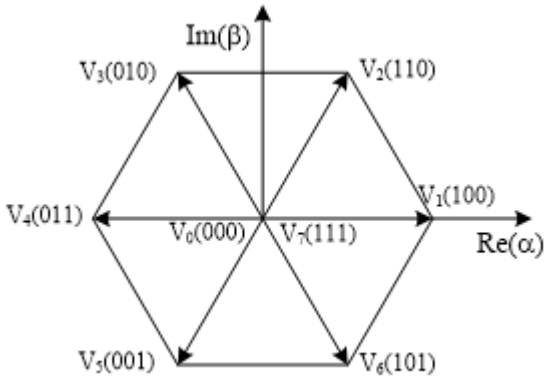

Figure 4. Space vector diagram.

The switching function vector ($\overrightarrow{S}$) can then be written as

$$\vec{S} = \frac{2}{3}\left(S_a + \vec{\omega}S_b + \overrightarrow{\omega^2}S_c\right) \tag{13}$$

while the rectifier's space vector ($\overrightarrow{V_{AFE}}$) related to phase to neutral voltages (v_{a0}, v_{b0}, v_{c0}) and dc bus voltage (V_{dc}) can be written as [19],[21]

$$\overrightarrow{V_{AFE}} = \frac{2}{3}\left(v_{a0} + \vec{\omega}v_{b0} + \overrightarrow{\omega^2}v_{c0}\right) \tag{14}$$

$$\overrightarrow{V_{AFE}} = \vec{S} \cdot V_{dc} \tag{15}$$

The relationship between the generated three-phase voltage vectors and the rectifier's input voltage vectors can be obtained by applying Kirchhoff's voltage law to the input side of the rectifier as

$$\vec{v}_s = L_s \frac{\vec{di}_s}{dt} + \mathrm{R}s\vec{i}_s + \frac{2}{3}\left(v_{a0} + \vec{\omega}v_{b0} + \overrightarrow{\omega^2}v_{c0}\right) - \frac{2}{3}\left(v_{n0} + \vec{\omega}v_{n0} + \overrightarrow{\omega^2}v_{n0}\right) \tag{16}$$

The input current dynamics of the rectifier, derived from (14), (16) and assuming $\frac{2}{3}\left(v_{n0} + \vec{\omega}v_{n0} + \overrightarrow{\omega^2}v_{n0}\right) = v_{n0}\,\frac{2}{3}\left(1 + \vec{\omega} + \overrightarrow{\omega^2}\right) = 0$, can be written as [19]

$$\frac{\vec{di}_s}{dt} = -\frac{R_s}{L_s}\vec{i}_s + \frac{1}{L_s}\vec{v}_s - \frac{1}{L_s}\overrightarrow{V_{AFE}} \tag{17}$$

The MPC is formulated in the discrete-time domain and thus, the rectifier's input current and rectified voltage are derived in a discrete-time model as in (18), using Euler's approximation in one switching period where T_s is the sampling time ($T_s > 0;\ k\mathrm{T}_s \le t \le (k+1)\mathrm{T}_s$) and k is the sampling instance.

$$\frac{\overrightarrow{di_s}}{dt} \approx \frac{\vec{\imath}_s\,(k+1) - \vec{\imath}_s\,(k)}{T_s} \tag{18}$$

For the $(k+1)$sampling instance the input current can be written as in (19) [18],[19],[21]

$$\vec{\imath}_s\,(k+1) = \left(1 - \frac{R_s T_s}{L_s}\right)\vec{\imath}_s(k) + \frac{T_s}{L_s}\left(\vec{v}_s(k) - \vec{v}_{AFE}(k)\right) \tag{19}$$

4.2. Finite Control Set MPC (FCS-MPC)

FCS-MPC with short prediction horizon is a promising control technology for achieving accurate control of the turbine speed through the control of the rectifier. MPC is used over many other control schemes for power converters such as PI, fuzzy, adaptive, sliding mode, etc. due to its simplicity and fast response. In this control scheme, a model of the system is considered in order to predict the future behavior of the variables [18]. According to [19], the MPC controllers is not only simpler than voltage oriented control based pulse width modulators but also accurately track the reference value by generating the optimum switching signal. Also, the MPC algorithm is easy to configure with constraints and non-linearity [18],[19]. The FCS-MPC requires high processing power and high accuracy of model parameters. At present, powerful processors overcome this issue at high speed and reduced cost [21].

The proposed control structure is designed to maintain the turbine speed at 650rpm. The FCS-MPC algorithm minimizes the error between reference and predicted angular speeds, denoted respectively by ω^* and ω^pwhich is calculated from

$$\omega^p = \omega_m(k+1) = \omega_m(k) + \frac{\mathrm{T}_s}{\mathrm{J}}\,(\mathrm{T}_m - \mathrm{T}_e) \tag{20}$$

In the control system, the future value of current, $i_s(k+1) = i_s^p$ is calculated from measured $v_s(k)$, $i_s(k)$ and $V_{dc}(k)$ by MPC controller using (19) for each one of eight possible switching vectors ($\vec{S}$). Then, i_s^p is converted into dq frame (i.e., i_d^p and i_q^p) to calculate ω^p of the turbine rotor, before it is compared to ω^* using the cost function of (g) from (21) to select the switching state which minimizes the cost function. The error between d axis current reference ($i_d^* = i_{d\_ref}\ (k+1)$) and predicted d axis current ($i_q^p = i_q(k+1)$) is added to the cost function with an arbitrary constant K to reduce the d-axis current in the generator and thereby avoid flux weakening. Figure 5 illustrates the proposed FCS-MPC control algorithm for the rectifier.

$$g = \left|\omega^* - \omega^p\right| + K.\left|i_d^* - i_d^p\right| \tag{21}$$

5. Simulation Results

A simulation study was carried out in MATLAB/Simulink to verify the operation of the proposed FCS-MPC based controller. Figure 3 illustrates the simulation model of proposed air turbine generator-dc grid integration system. The simulation results are shown in Figure 6(a)-6(h) which are used to verify the operation of the proposed controller. Figure 6(a) shows the torque profile applied to the generator [7]. Figure 6(b) depicts the q axis stator current which varies in proportion to the torque. Figure 6(c) shows the active power and reactive power output of the generator. The active power also varies in proportion to the torque which confirms the ability of the proposed controller to extract power from OWC air turbine with varying input torque. Figure 6(d) shows the rotor angular speed is

following the reference value 68rad/s which is set at target operating conditions of the air turbine. As shown in Figures 6(e-f), the PMSG's output voltage and current are nearly sinusoidal. As shown in Figure 6(g) the total harmonic distortion (THD) of the *a*-phase current (i_a) is less than 5% which complies with the IEEE standards [22]. Figure 6(h) illustrates the dc bus voltage which has only 2% variation.

6. Conclusions

This paper presents an MPC-based speed controller for an air turbine-connected PMSG of an oscillating water column WEC system. Simulation results verify the that the proposed controller is able to extracting power from the turbine at varying input torque conditions while maintaining the speed at the set point. The proposed controller does not require tuning and thus, it is easy to implement. The discrete nature of the controller makes it easy to realize in modern digital controllers.

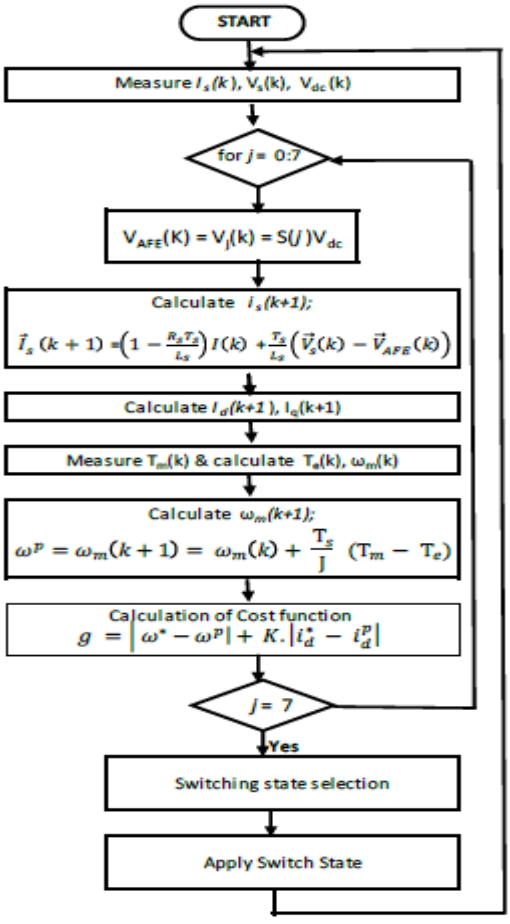

Figure 5. Proposed FCS-MPC algorithm flowchart for the rectifier.

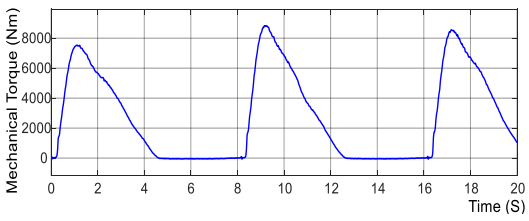

(a) Mechanical torque T_m (Nm)

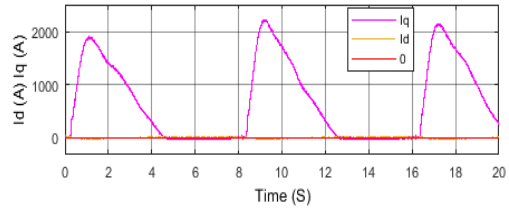

(b) I_d and I_q components of stator current in the *dq* frame

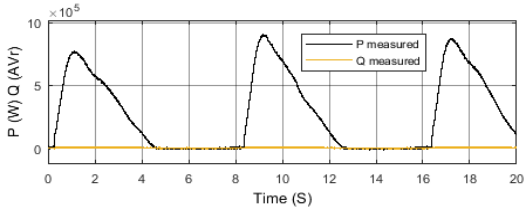

(c) Active power P (W) and reactive power Q (Var) of the PMSG

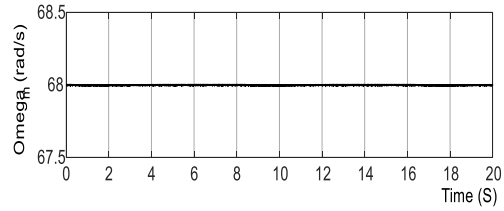

(d) Rotor angular speed $Omega_m$ (rad/s)

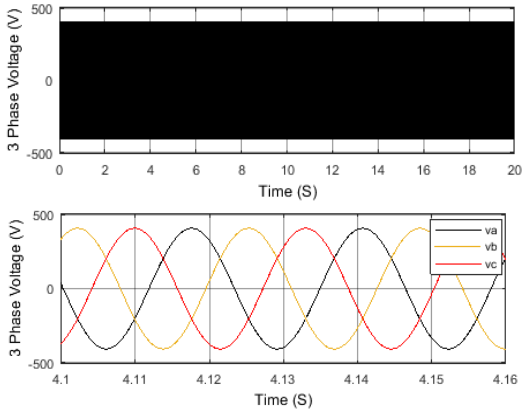

(e) Generator output voltage V_{abc} (V)

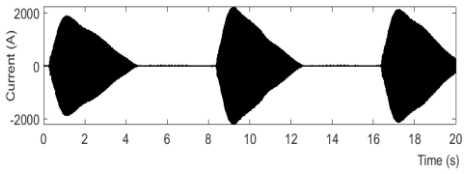

(f) Stator current – i_{abc} (A)

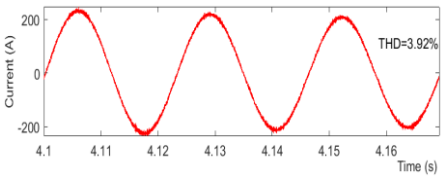

(g) Stator current i_a

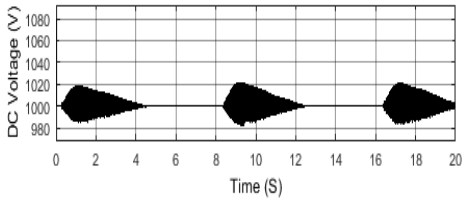

(h) dc link voltage V_{dc} (V)

Figure 6 (a) – 6 (h). Performance of the proposed FCS-MPC for the PMSG of an OWC unidirectional air turbine.

Acknowledgement
The authors thank Wave Swell Energy for providing the parameters to use in the simulation studies.

Reference

[1] Australian Government, Department of Industry, Geoscience Australia, Bureau of Resources and Energy Economics. (2010). *Australian Energy Resource Assessment 2010*.
[2] M. G. Hughes and A. D. Heap, "National-scale wave energy resource assessment for Australia," *Renewable Energy*, vol. 35, pp. 1783–1791, 2009.
[3] Australian Government, Department of Industry, Geoscience Australia, Bureau of Resources and Energy Economics. (2014). *Australian Energy Resource Assessment 2014*.
[4] "World Energy Resources Marine Energy " *World Energy Council World Energy Resources 2016*, no. 24, 2016.
[5] S. Benelghali, M. E. H. Benbouzid, and J. F. Charpentier, "Marine Tidal Current Electric Power Generation Technology: State of the Art and Current Status.," in *IEEE IEMDC'07*, Antalya, Turkey, 2007, no. May 2007, pp. 1407-1412: IEEE, 2007.
[6] *Oceanlinx*. Available: http://www.oceanlinx.com/
[7] *Wave Swell Energy*Available: http://waveswellenergy.com.au/
[8] Y. Hong, R. Waters, C. Boström, M. Eriksson, J. Engström, and M. Leijon, "Review on electrical control strategies for wave energy converting system," *Renewable and Sustainable Energy Reviews*, pp. 329–342, 2014.
[9] *BPS Renewable Energy Company*Available: bps.energy/projects
[10] *Carnegie Clean Energy* Available: http://carnegiewave.com/
[11] M. Takao and T. Setoguchi, "Review Article Air Turbines forWave Energy Conversion," *International Journal ofRotating Machinery*, 2012.
[12] T. Setoguchi, S. Santhakumar, H. Maeda, and K. Kaneko, "A review of impulse turbines for wave energy conversion," *Renewable Energy* vol. 23, pp. 261–292, 2001.
[13] S. Benelghali, M. E. H. benbouzid, and J. F. Charpentier, "Generator Systems for Marine Current Turbine Applications: A Comparative Study," *IEEE Journal of Oceanic Engineering*, vol. 37, no. 3, pp. 554-563, July 2012 2012.
[14] D. L. O'Sullivan and A. W. Lewis, "Generator Selection and Comparative Performance in Offshore Oscillating Water Column Ocean Wave Energy Converters," *IEEE Transactions on Energy Conversion*, vol. 26, 2011.
[15] M. Abdelrahem, C. Hackl, and R. Kennel, "Model Predictive Control of Permanent Magnet Synchronous Generators in Variable-Speed Wind Turbine Systems," presented at the Power and Energy Student Summit 2016 (PESS 2016), 2016.

[16] A. Hansen, F. Iov, F. Blaabjerg, and L. Hansen, "Review of contemporary wind turbine concepts and their market penetration," *Journal of Wind Energy*, vol. 58, pp. 1081-1095, April 2011 2011.

[17] L. B. Xie and T. H. Tang, "Modeling and Control of a Small Marine Current Power Generation System," (in English), *2012 IEEE International Symposium on Industrial Electronics (Isie)*, no. 28-31 May 2012, pp. 1438-1443, 12 July 2012 2012.

[18] J. Rodriguez *et al.*, "State of the Art of Finite Control Set Model Predictive Control in Power Electronics," *IEEE Transactions on Industrial Informatics*, vol. 9, pp. 1003-1016, May 2013 2013.

[19] M. Parvez, N. M. L. Tan, and H. Akagi, "An Improved Active-Front-End Rectifier Using Model Predictive Control," presented at the IEEE App. Power Electro. Conf. and Expo. (APEC), 2015.

[20] R. Krishnan, *Permanent magnet synchronous and brushless DC motor drives*. Taylor & Francis Group, London, 2010.

[21] Z. Liu, D. Wang, and Z. Peng, "A Simplified Direct Finite-Control-Set Model Predictive Control for AFEs with DC-Link Voltage Dynamic Reference Design," presented at the 35th Chinese Control Conference (CCC), Chengdu, China, 2016.

[22] "IEEE Recommended Practice and Requirements for Harmonic Control in Electric Power Systems," vol. Revision of IEEE Std 519-1992, 2014.